

NASA Technical Paper 1584

LOAN COPY: RETURN
AFWL TECHNICAL LIBRARY
WRIGHT PATTISON AFB, N. M.



Lubrication and Wear Mechanisms of Polyimide-Bonded Graphite Fluoride Films Subjected to Low Contact Stress

Robert L. Fusaro

JANUARY 1980





NASA Technical Paper 1584

Lubrication and Wear Mechanisms of Polyimide-Bonded Graphite Fluoride Films Subjected to Low Contact Stress

Robert L. Fusaro
Lewis Research Center
Cleveland, Ohio



National Aeronautics
and Space Administration

**Scientific and Technical
Information Office**

1980

SUMMARY

The tribological properties of polyimide-bonded graphite fluoride films were studied with a pin-on-disk friction apparatus. But instead of sliding a hemispherically tipped pin against the film (as is normally done), a flat pin was used. A 0.95-millimeter-diameter flat (7.1×10^{-3} -cm² area) was first generated on a 0.476-centimeter-radius hemispherically tipped AISI 440C HT stainless-steel rider before it was slid against the film under a 1-kilogram load. This load was projected to give a contact stress of 14 megapascals (2000 psi). The film completely supported this load, and the wear process was one of gradual wear through the film: It took approximately 3500 kilocycles of sliding to wear through the 45-micrometer-thick film.

The lubricating mechanism during this stage appeared to be the plastic flow, or shearing, of a thin surface layer of the film between the rider and the bulk of the film. The plastic flow extended to a depth of less than 2 micrometers, and the layer tended to become textured. Repeated passes over the film caused this textured layer to blister and spall from the surface in localized areas. Spalling of very thin layers appeared to be the major mechanism of film wear; however, some thicker particles and pits (~ 6 μm thick) were also observed. These were postulated to be caused by cracks propagating through the bulk film below the surface layer on the wear track.

Once the bonded film had worn through to the metallic substrate, the lubricating mechanism consisted of the shear of very thin lubricant films (< 0.4 μm) between flat plateaus generated on the sandblasted asperities of the metallic substrate and the flat area on the rider. Lubricant was supplied from the valleys between the asperities or from the sides of the wear track.

During the first lubrication stage (no metallic asperity contact), no measurable wear to the rider occurred; but during the second stage (metallic asperity contact), rider wear increased gradually with sliding distance.

INTRODUCTION

The friction, film wear life, and rider wear for AISI 440C HT stainless-steel riders sliding on polyimide-bonded graphite fluoride films have been previously studied with a pin-on-disk friction apparatus (refs. 1 and 2). Long wear lives (~ 3000 kilocycles of sliding) and low friction coefficients (0.12 to 0.20) were obtained at 25^o C in a moist

air atmosphere (50 percent relative humidity). Rider wear rates were also very low (3.4×10^{-17} to 4.7×10^{-17} m³/m; ref. 3).

In a Falex testing apparatus, similarly formulated films failed after 15.8 minutes (4.6 kilocycles) of sliding (ref. 4). The authors of reference 4 have attributed this short wear life to the films' load-carrying capacity. That is, they were not suitable for the highly concentrated loads (≤ 227 kg (500 lb)) applied in those experiments.

Although there are many applications for solid lubricants where high loads are used, there are also many applications for lighter loads. One example is in foil bearings, where loads of less than 2.6×10^2 kilopascals (37 psi) are typical (ref. 5). Thermal exposure experiments on polyimide-bonded graphite fluoride films (ref. 3) show that this lubricant has a higher thermal stability than the PTFE solid lubricant presently used in foil bearings. There is an advantage in operating these bearings at temperatures higher than those at which they are presently used, and polyimide-bonded graphite fluoride has potential for this application.

It would be beneficial to know if the longer wear lives obtained with the pin-on-disk tester (compared to those obtained with the Falex tester) were due simply to load capacity or to other factors that are involved with the mechanisms by which bonded solid lubricant films lubricate, wear, and fail. In an earlier study (ref. 6), the lubricating and wear mechanisms for a hemispherically tipped rider (0.476-cm radius) sliding on polyimide-bonded graphite fluoride films were determined. In general, two stages of lubrication were identified. In the first stage, the film itself supported the load and the lubricating mechanism appeared to be the shear (plastic flow) of a thin surface layer of the film between the bulk of the film and the metallic rider. In the second stage (which occurred after the original film had worn through to the metallic substrate), the lubricating mechanism appeared to be the shear of very thin lubricant films between the flat area on the rider and flat plateaus generated on the metallic asperities in the film wear track.

For the hemispherically tipped rider sliding on the film, the first stage of lubrication lasted only a very short time (<15 kilocycles of sliding). From rider contact area measurements, the projected contact stress after 1/4 kilocycle of sliding was 170 megapascals (25 000 psi); and although the Hertz stress was not calculated, it would have been even higher. Since the hemispherically tipped rider sliding on the film imparted such high initial stresses, this study was conducted to determine if a lower contact stress would alter the lubricating and wear mechanisms of polyimide-bonded graphite fluoride films. This objective was met by generating a 0.95-millimeter-diameter flat on the (0.476-cm-radius) hemispherically tipped rider before sliding it against the film. A 1-kilogram load was applied to the flat to obtain a projected contact stress of 14 megapascals (2000 psi). Wear life, friction coefficient, film wear, and rider wear

were evaluated for a 45-micrometer-thick film. These results were then compared with those obtained for the hemispherical contact geometry as reported in reference 6.

MATERIALS

Pyralin polyimide (PI-4701) was used in this study. The polyimide was obtained as a thick precursor solution containing 43 percent solids. For a sprayable mixture, a thinner consisting of N-methyl-pyrrolidone and xylene was added to it. The polyimide-bonded graphite fluoride films were prepared by mixing equal parts by weight of polyimide solids with graphite fluoride powder. The graphite fluoride used had a fluorine-carbon ratio of 1.1. The films were applied to AISI 440C HT steel disks (1.2 cm thick by 6.3 cm in diam) that had a hardness of Rockwell C-58. The riders used in the friction and wear tests were also made from the AISI 440C HT steel with a hardness of Rockwell C-58.

FRICITION APPARATUS

A conventional pin-on-disk friction and wear apparatus was used in this study (fig. 1), except that before the experiments, a 0.95-millimeter-diameter flat was worn on the 0.476-centimeter-radius hemispherically tipped rider (pin) by sliding it against a graphite fluoride film rubbed on a sandblasted disk. The rider was not removed from the holder during cleaning, and it and the disk (with applied polyimide-bonded graphite fluoride film) were positioned (and indexed) in the apparatus by using a linear variable differential transformer (LVDT) so that a flat-on-flat configuration was produced with minimal misalignment.

A 1-kilogram load applied to the flat on the rider gave a projected contact stress of 14 megapascals (2000 psi) against the film. The disk was 6.3 centimeters in diameter, and the rider slid on the disk at a radius of 2.5 centimeters. The disk was rotated at 1000 rpm, for a linear sliding speed of 2.6 meters per second. The friction specimens were enclosed in a chamber so that the atmosphere could be controlled. The controlled air atmosphere of 10 000 ppm H₂O (~50 percent relative humidity) was achieved by mixing dry air with dry air bubbled through water. These experimental conditions, except for the projected contact stress, were the same as those used in reference 6.

PROCEDURE

Surface Preparation and Cleaning

The disk surfaces were roughened by sandblasting to a centerline average (cla) roughness of 0.9 to 1.2 micrometers. After surface roughening, the disks were scrubbed with a brush under running tap water to remove the abrasive particles. A water paste of levigated alumina was next rubbed over the surface with a polishing cloth. (Cleaning with levigated alumina did not change surface roughness.) This was followed by a second scrubbing under running tap water. The disks were rinsed in distilled water and then clean, dry compressed air was used to quickly dry the surfaces. The disks were stored in a dessicator until they were ready for coating with the solid lubricant.

The rider was lightly scrubbed with ethyl alcohol and with levigated alumina to remove from the flat the graphite fluoride transfer film that originated during the flat's generation. It was next rinsed in distilled water and dried with compressed air. Lubricant was not applied to the riders.

Film Application

The polyimide-bonded graphite fluoride films were applied to the disks with an artist's airbrush. Because the films did not dry rapidly, only a thin layer was applied at one time in order to prevent "running." Each thin layer was cured completely before the next layer was applied. The cure consisted of heating the films at 100^o C for 1 hour and then at 300^o for 2 hours.

The film thickness evaluated in this study was 45 micrometers (0.0018 in.). Since each layer applied was from 8 to 13 micrometers thick, four applications were needed to achieve the desired thicknesses.

Friction and Wear Tests

The procedure for conducting the friction and wear tests was as follows: A rider and disk (with applied solid lubricant film) were inserted into the friction apparatus, and the test chamber was sealed. The atmosphere was controlled by purging moist air (10 000 ppm H₂O) through the chamber for 15 minutes before each test. The moist air flow was continued throughout the test at a flow rate of 1500 cubic centimeters per minute. The volume of the chamber was 2000 cubic centimeters. After the chamber was purged for 15 minutes, the disk was set into rotation at 1000 rpm and a 1-kilogram load was gradually applied. The test temperature was 25^o C.

Each test was stopped after 1 kilocycle (1 min) of sliding. After the rider and disk were removed from the friction apparatus, the contact areas were examined by optical microscopy and photographed. Surface profiles of the disk wear tracks were also taken. The rider and disk were then placed back into the apparatus, and the test procedure was repeated. The rider was not removed from the holder, and locating pins in the apparatus insured that it was returned to its original position. The same was true for the disk.

Each test was stopped and the test procedure repeated after sliding times of 1, 15, 60, 250, 500, 1500, 2500, 3500, 4500, 6000, and 8500 minutes. Film wear was calculated by measuring the cross-sectional area of the polyimide-bonded graphite fluoride film wear track (from the surface profiles) after each sliding interval. Rider wear was determined by measuring the change in the diameter of the wear scar on the hemispherically tipped rider and then calculating the volume of material worn away.

Analysis of Sliding Surfaces

Optical microscopy techniques were used to study the lubricating films, the transfer films, and the wear particles in this investigation. The surfaces were viewed at magnifications to 1100. At these high magnifications, the depth of field was very small ($\sim 1 \mu\text{m}$); thus the focusing distance was used in measuring the various features on the sliding surfaces, such as film thickness and wear track depth.

The thin films ($1 \mu\text{m}$ or less) of polyimide-bonded graphite fluoride were transparent. Since illumination and observation of the surfaces were normal to the surfaces, interference fringes could be seen in the films both on the disk wear track and on the rider. Interference fringes indicated that solid lubricant films were present and that the films were smooth and continuous.

A surface profilometer was used to obtain surface profiles of the film wear track after various sliding intervals. At least four profiles were taken at each interval. From these profiles, the cross-sectional area of film wear was determined at each sliding interval. These areas were then plotted as a function of sliding distance (or time) in order to determine a film wear rate.

Since the surface of the film was very rough, the rider initially only made contact on the highest film asperities. These areas became bright and shiny. Thus a quantitative metallurgical system (QMS), which is an image analysis technique, was used to determine the percentage of the wear track that had the shiny appearance. By assuming that full contact was occurring on the shiny areas, the contact stress on the asperities was estimated.

RESULTS AND DISCUSSION

Friction and Wear Life

A friction trace for a 0.95-millimeter-diameter flat sliding against a polyimide-bonded graphite fluoride film is shown in figure 2. The friction trace is shown discontinuously because the tests were stopped at the indicated intervals to make wear measurements and to observe the sliding surfaces with an optical microscope. As had been found for the hemispherically tipped rider sliding on the same film (ref. 6), the friction coefficient started at a low value of 0.08 to 0.09, then rose gradually with sliding distance, and eventually leveled off at 0.24 ± 0.02 . This was slightly higher than the friction coefficient found in reference 6 (0.20 ± 0.02).

Wear life for AISI 440C HT riders sliding against polyimide-bonded graphite films applied to AISI 440C HT substrates has been defined as the number of sliding revolutions to reach a friction coefficient of 0.30 (ref. 6). Optical microscopy of the sliding surfaces indicated that this is a good choice. When the friction coefficient reached this value, the film wear track had become depleted of solid lubricant and both the rider and the film wear track were covered with powdery films that were very different from the thin, flowing films found when good lubrication occurred.

For the 0.95-millimeter-diameter flat sliding on the 45-micrometer-thick film, failure did not occur after 8500 kilocycles of sliding (which was the time duration of the test).

Film Wear

Film wear was studied by taking surface profiles of the film wear track after each sliding interval. Figure 3 gives typical surface profiles after sliding intervals of 15, 500, 1500, 3500, and 8500 kilocycles. Because the vertical magnification of the surface profiles is about 50 times the horizontal magnification, the view of the surface is distorted.

The surface profiles indicate that the wear process was one of gradual wear through the film. It took approximately 3500 kilocycles for the rider to wear through the 45-micrometer-thick film and make contact with the sandblasted metallic substrate. Once the metallic substrate was reached, there was a gradual increase in wear track width.

To quantify the wear process, we calculated film wear (for the first 3500 kilocycles of sliding) by measuring the cross-sectional area of the film wear tracks (from the surface profiles) after each sliding interval. At least four traces were taken at each interval. Figure 4 plots the average and the range of these values as a function of the

number of sliding revolutions (expressed in kilocycles). The general trend was that the film wear increased linearly (from zero) as a function of sliding revolutions. A linear regression fit (least squares) of the points gave an average film wear rate of $(1.7 \pm 0.3) \times 10^{-7} \text{ cm}^2/\text{kilocycle}$, or in terms of wear volume per unit of sliding distance the average wear rate was $(1.7 \pm 0.3) \times 10^{-14} \text{ m}^3/\text{m}$. The wear rate for the hemispherically tipped rider sliding on the film (ref. 6) was $(1.2 \pm 0.4) \times 10^{-11} \text{ m}^3/\text{m}$. Thus, wear was reduced about 1000 times at the lower contact stress with a flat rider.

Film Wear Mechanisms

Film wear was also studied with an optical microscope to magnifications of 1100. Figure 5 gives photomicrographs of the film wear track after sliding intervals of 1, 15, 60, and 250 kilocycles. The photomicrographs illustrate that during the first 250 kilocycles of sliding, the rider only contacted the film on the tips of the film asperities. The bright areas in the photomicrographs of figure 5 are flat plateaus that were worn on the asperities of the polyimide-bonded film during the initial run-in. As repeated passes were made over the wear track, the ratio of bright area to dark area increased (fig. 5), an indication that the asperities were being truncated.

To quantify the contact stresses involved, we observed the wear track by using QMS. Table I shows how the estimated area of contact increased (in percent) as a function of sliding duration and the corresponding calculated stress. Figure 6 gives the estimated contact stress on the film asperities as a function of sliding duration. The stress was calculated by assuming that all bright areas were contacting the rider flat at any particular interval. However, this may not have been the case, and these values of contact stress may be low. Nevertheless, the data give an estimate of the contact stresses involved.

Assuming full contact on the film asperity tips, the rider contact after 1 kilocycle of sliding was estimated to be approximately 20 percent of full contact. Thus, the contact stress supported by the film asperities was at least 69 megapascals (10 000 psi). Because of film asperity wear, the contact stress dropped very rapidly during the first 15 kilocycles of sliding (fig. 6), to 42 megapascals (6100 psi). After 15 kilocycles of sliding the wear rate also decreased, and it took approximately 500 kilocycles of sliding to reach a steady-state value of approximately 17 megapascals (2500 psi). This represents a contact area of approximately 80 percent of full contact. Because of the mechanisms by which the film wore, full contact never occurred.

The wear progression of an individual film asperity is shown in figure 7 after sliding intervals of 1, 15, 60, and 250 kilocycles. The high-magnification photomicrographs show the truncation of the film asperity and its merging with other asperities as

truncation occurred. The plateau on the film asperity was very smooth and reflective; however, there were some very fine cracks and areas where the film has spalled from the plateau. High-magnification optical observation of the film wear track suggested that spalling of thin layers on the plateaus was the primary wear mechanism while sliding was on the film asperities (at least under the conditions used in this investigation).

After 500 kilocycles of sliding, the film asperities were worn away (fig. 3). As figure 3 shows, the rider continued to wear gradually through the film until the metallic asperities on the substrate were reached at approximately 3500 kilocycles of sliding. Figure 8(a) shows the film wear track after 1500 kilocycles of sliding, and figure 8(b) shows the film wear track after 3500 kilocycles of sliding. Very tiny bright spots can be seen in the film after 3500 kilocycles of sliding. These are the tips of the metallic asperities on the substrate.

The film wear mechanism (after the film asperities had been worn away) was very similar to the mechanism when sliding was only on the film asperity plateaus. Figure 9 shows two areas of the film wear track after 1500 kilocycles of sliding. In general, the track was smooth and lustrous, but there were blistered areas (figs. 9(a) and (b)) and areas where a very thin layer of film had spalled from the surface (fig. 9(b)) and exposed unrubbed polyimide-bonded graphite fluoride. The area exposed after the film had spalled was not lustrous and appeared rough. The thickness of the layers that spalled varied somewhat; usually they were less than 1 to 2 micrometers thick but occasionally they were as thick as 6 micrometers.

One mechanism by which spalling occurred appeared to be due to texturing of the wear track. Texturing means that the individual constituents (polyimide and graphite fluoride) plastically flowed and coalesced on the wear track into a very thin, smooth layer at the surface of the film. After repeated passes were made over this layer, it tended to disengage from the bulk film by blistering and spalling. Another wear mechanism (not shown in the figures) appeared to originate in the bulk of the film, since the textured layer was 1 to 2 micrometers thick and some spalled areas were as much as 6 micrometers thick. These spalled areas were most likely caused by crack propagation due to defects in the bulk; while the thinner spalled layers were caused by the scaling textured layer.

Lubricating Mechanisms

In the first stage of lubrication, wear occurred gradually through the film. The lubricating mechanism (as deduced by studying the sliding surfaces with optical microscopy) during this stage appeared to be the shear (plastic flow) of a thin surface layer of the film between the rider and the bulk of the film.

After the original film had been worn through to the metal surface, the second stage of lubrication began. In this stage, interaction of the rider flat with the asperities on the sandblasted metallic substrate caused flats to be worn on the tips of those asperities (figs. 8(b) to (d) and 10). The lubricating mechanism then became the shear of very thin lubricant films ($0.8 \mu\text{m}$) between the rider flat and the flat plateaus on the metallic asperities. Figure 10(b) shows very thin lubricant films on these plateaus.

The lubricant was supplied to the metallic plateaus from the valleys between the asperities or from the sides of the wear track. The thin lubricant films essentially flowed across the metallic plateaus and were deposited in a following valley. Figure 11, an idealized schematic drawing of the sliding surfaces, illustrates this lubricating mechanism.

Rider Wear and Transfer

A photomicrograph of the rider flat before sliding is shown in figure 12. Also shown in figure 12 is the same rider flat after sliding intervals of 1, 250, 1500, 4500, and 8500 kilocycles. Figure 12(b) shows that initially very thin transfer occurred on the rider flat. Figure 13(a) is a high-magnification photomicrograph of that transfer. Broad, colorful interference bands are visible. On continued sliding, the transfer to the rider gradually increased (figs. 12(b) to (d) and 13(a) to (c)). Comparing the friction trace of figure 2 with the amount of transfer suggests that the friction was lowest when the transfer was thinnest.

Transfer may not have been the only reason for the increase in friction coefficient between 0 to 250 kilocycles of sliding. Figure 5 and table I indicate that the contact area and the contact pressure were continuously changing during the sliding interval of 0 to 250 kilocycles. This may have also affected the friction coefficient and the resultant amount of transfer.

After approximately 3500 kilocycles of sliding, the bonded film was worn away and contact had been made with the metallic asperities. When this occurred, the transfer film began to thin from the scouring action of the metallic asperities. Since the metallic asperity tips were exposed to the rider gradually, the transfer film thinned very slowly (figs. 12(e) and (f)). For the same reason, the rider did not show any measurable wear until after 4500 kilocycles of sliding.

The rider wear rate for the duration of the experiment was calculated and compared with that for the experiment in which a hemisphere slid on the film (ref. 6). Those data are shown in table II. From 4500 to 6000 kilocycles of sliding the wear rate for the flat sliding on the film ($0.0032 \times 10^{-15} \text{ m}^3/\text{m}$) was much less than that for the hemisphere sliding on the film; however, for 6000 to 8500 kilocycles the flat-rider

wear rate ($0.021 \times 10^{-15} \text{ m}^3/\text{m}$) correlated very well with the steady-state hemispherical-rider wear rate (table II).

Very little wear occurred to the rider for sliding intervals up to 6000 kilocycles, most likely because enough lubricant was present to negate the scouring effect of the metallic asperities. Only when sufficient lubricant depletion occurred did the metallic asperities scour the rider and increase wear.

Thin transfer films were found on the rider after 6000 and 8500 kilocycles of sliding (figs. 12(f) and 13(d)); however, they looked somewhat different than the thin transfer films found after 1 kilocycle of sliding (figs. 12(b) and 13(a)). Interference fringes were only visible in the entrance of the rider contact area (fig. 13(d)); and the transfer in the contact area itself was milky colored, an indication that the transfer was thinner than the wavelength of light ($0.4 \mu\text{m}$).

SUMMARY OF RESULTS

Friction, wear, surface profilometry, and optical microscopy studies of a polyimide-bonded graphite fluoride film subjected to sliding against a flat 440C HT stainless-steel surface had the following results:

1. Two stages of lubrication were operating (as was observed for hemispherical contact):

a. In the first stage the film itself supported the load and the lubricating mechanism was the shear (plastic flow) of a thin surface layer of the film between the rider and the bulk of the film.

b. The second stage began after the original film had worn away and consisted of the shear of thin films of polyimide-bonded graphite fluoride between the flat rider and flat plateaus generated on the metallic asperities of the substrate.

2. Two wear mechanisms operated during the first stage of lubrication:

a. The first mechanism was spalling of the textured surface layer (wear particles less than $2 \mu\text{m}$ thick).

b. The second mechanism was crack propagation in the film below the textured layer (wear particles greater than $2 \mu\text{m}$ thick).

3. Reducing contact stress (for the same total load) markedly reduced the film wear rate and increased the film wear life. The hemisphere wore through the film after 15 kilocycles of sliding at a rate of $(1.2 \pm 0.4) \times 10^{-11} \text{ m}^3/\text{m}$. The flat wore through the film after 3500 kilocycles of sliding at a rate of $(1.7 \pm 0.3) \times 10^{-14} \text{ m}^3/\text{m}$.

4. During the first stage of lubrication, no measurable wear of the rider occurred; but after transition to the second stage, rider wear increased with sliding distance.

The rider wear rate of the hemisphere and the flat were very similar (2.5×10^{-17} and 2.1×10^{-17} m³/m).

5. On initial rider contact with the film, the tips of the film asperities supported the load. Assuming that all tips contacted the rider, the calculated load on the film asperities after 1 kilocycle of sliding was 69 megapascals (10 000 psi).

Lewis Research Center,
National Aeronautics and Space Administration,
Cleveland, Ohio, August 13, 1979,
505-04.

REFERENCES

1. Fusaro, Robert L.; and Sliney, Harold E.: Lubricating Characteristics of Polyimide Bonded Graphite Fluoride and Polyimide Thin Films. Trans. ASLE, vol. 16, no. 3, July 1973, pp. 189-196.
2. Fusaro, Robert L.; and Sliney, Harold E.: Graphite Fluoride as a Solid Lubricant in a Polyimide Binder. NASA TN D-6714, 1972.
3. Fusaro, Robert L.: Effect of Thermal Exposure on Lubricating Properties of Polyimide Films and Polyimide-Bonded Graphite Fluoride Films. NASA TP-1125, 1978.
4. McConnell, B. D.; Snyder, C. E.; and Strang, J. R.: Analytical Evaluation of Graphite Fluoride and Its Lubrication Performance Under Heavy Loads. Lubr. Eng., vol. 33, no. 4, Apr. 1977, pp. 184-190.
5. Koepsel, Warren F.: Gas Lubricated Foil Bearing Development for Advanced Turbomachines. Vol. 1: Technical Discussion. AIRESEARCH-76-312202-1, AiResearch Mfg. Co., 1977. (AFAPL-TR-76-114-Vol-1, AD-A042980.)
6. Fusaro, Robert L.: Lubricating and Wear Mechanisms for a Hemisphere Sliding on Polyimide-Bonded Graphite Fluoride Film. NASA TP-1524, 1979.

TABLE I. - EFFECT OF SLIDING DURATION ON
ESTIMATED AREA OF CONTACT AND
RESULTANT CONTACT STRESS

[0.95-mm-diam flat (7.1×10^{-3} -cm² area) sliding on polyimide-bonded graphite fluoride film under 1-kg load. Percent area of contact determined by using a QMS image analysis system.]

Sliding interval, kilocycles	Estimated area of contact, percent	Contact stress	
		MPa	psi
1	20	69	10 000
15	33	42	6 100
60	37	37	5 400
250	60	23	3 300
500	80	17	2 500
1500	80	17	2 500

TABLE II. - EFFECT OF TYPE OF CONTACT ON
RIDER WEAR RATE

[Riders sliding against 45- μ m-thick polyimide-bonded graphite fluoride film applied to sandblasted 440C HT stainless-steel disk.]

Sliding interval, kilocycles	Type of film contact	
	Hemisphere ^a	0.95-mm-diameter flat on hemisphere
	Rider wear rate, m ³ /m	
0 to 1	0	0
1 to 5	0	↓
5 to 15	0	
15 to 60	0.069×10^{-15}	
60 to 250	$.032 \times 10^{-15}$	
250 to 500	$.025 \times 10^{-15}$	
500 to 900	$.047 \times 10^{-15}$	
900 to 1800	$.330 \times 10^{-15}$	
1800 to 3800	$.640 \times 10^{-15}$	
3800 to 4500	^b $.880 \times 10^{-15}$	
4500 to 6000	-----	
6000 to 8500	-----	$.0210 \times 10^{-15}$

^aData from ref. 6.

^bFailure (a friction coefficient of 0.30) occurred at 4400 kilocycles.

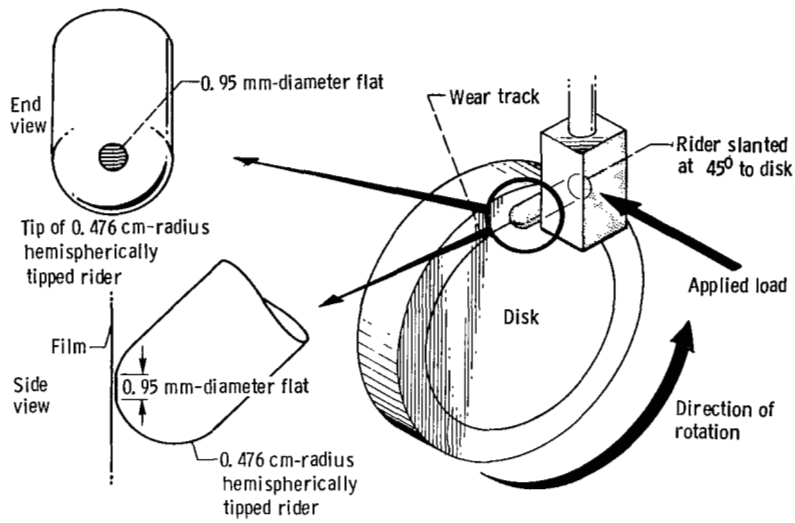


Figure 1. - Schematic arrangement of friction specimens.

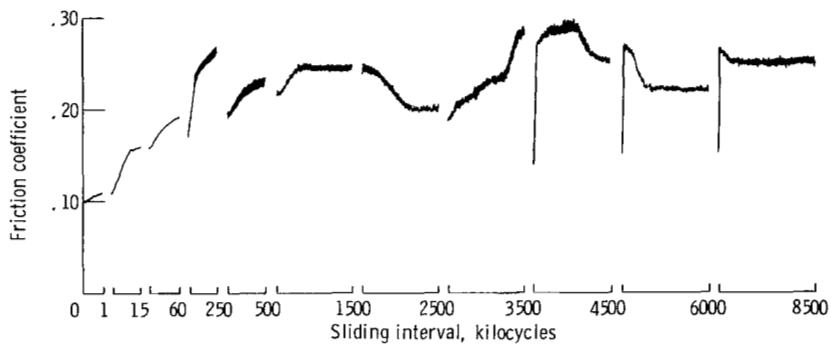


Figure 2. - Friction trace for 440C HT stainless-steel rider (with 0.95-mm-diam flat) sliding on polyimide-bonded graphite fluoride film. Load, 1 kilogram; speed, 2.6 meters per second; test temperature, 25° C; test atmosphere, moist air (10 000 ppm H₂O).

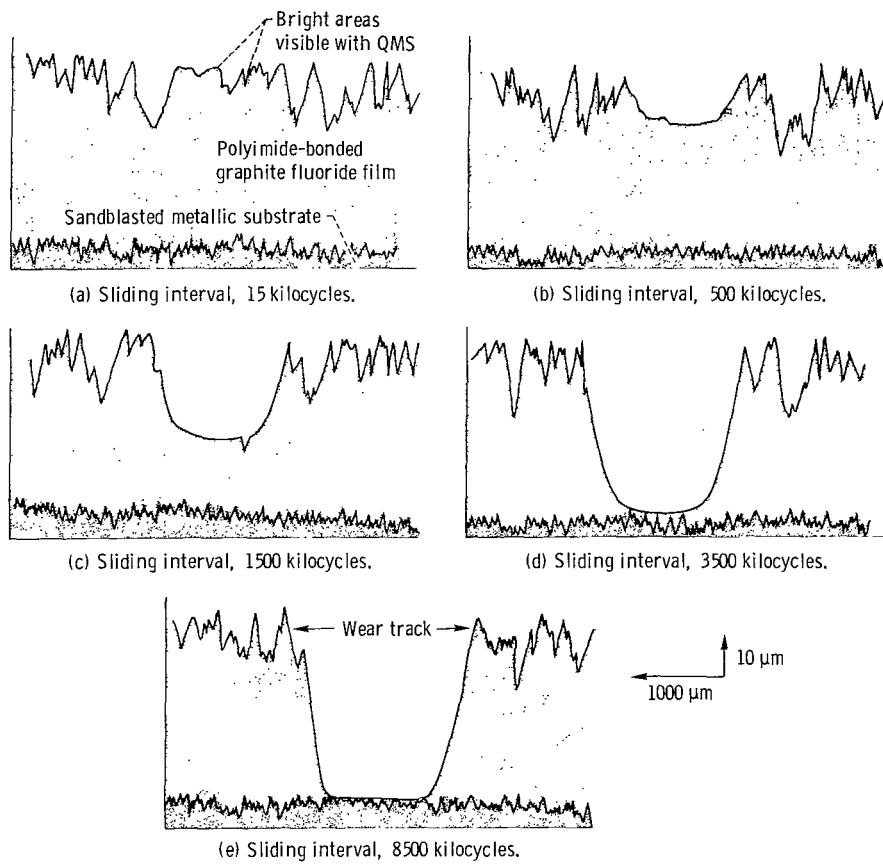


Figure 3. - Surface profiles taken after various sliding intervals for 0.95-mm-diameter flat sliding on polyimide-bonded graphite fluoride film. Rider and disk substrate, 440C HT stainless steel; load, 1 kg; estimated contact stress, 14 MPa (2000 psi); sliding speed, 2.6 m/sec; temperature, 25^o C; atmosphere, moist air (10 000 ppm H₂O).

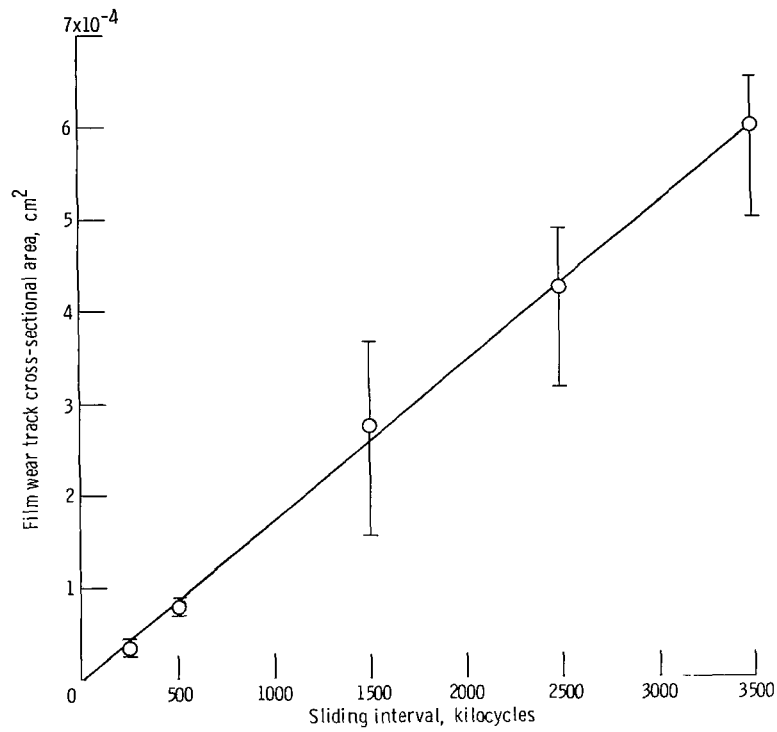
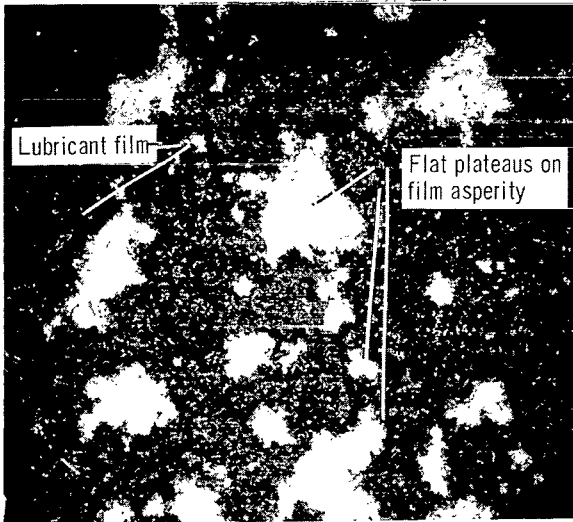
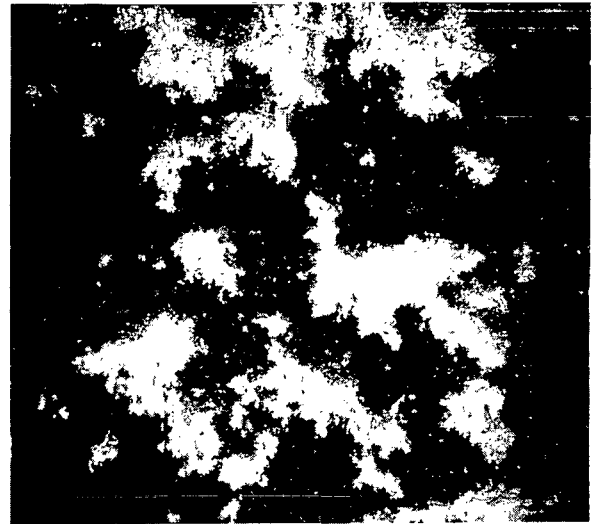


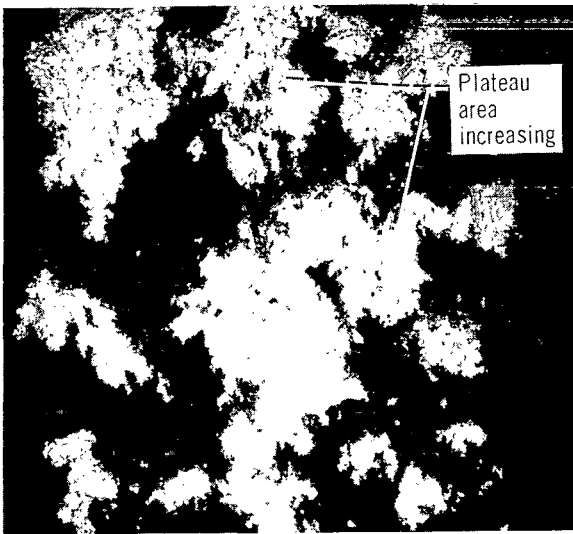
Figure 4. - Wear of polyimide-bonded graphite fluoride film as function of sliding interval. Rider and substrate material, 440C HT stainless steel; load, 1 kg; projected contact stress, 14 MPa (2000 psi); sliding speed, 2.6 m/sec; temperature, 25° C; atmosphere, moist air (10 000 ppm H₂O).



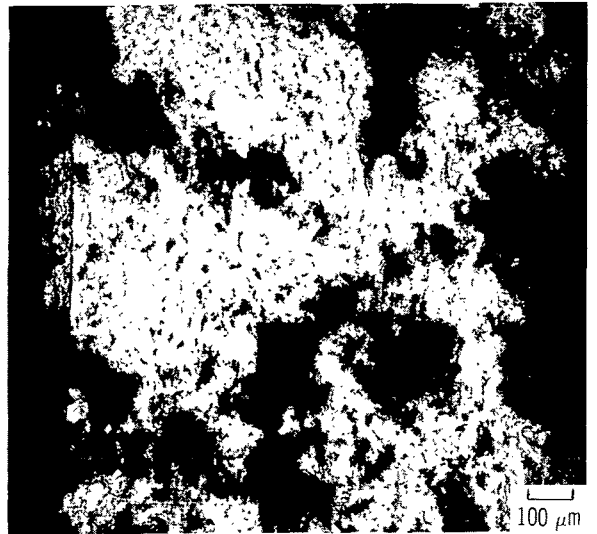
(a) Sliding interval, 1 kilocycle.



(b) Sliding interval, 15 kilocycles.



(c) Sliding interval, 60 kilocycles.



(d) Sliding interval, 250 kilocycles.

Figure 5. - Photomicrographs of wear tracks on polyimide-bonded graphite fluoride films after various sliding intervals. Rider and disk substrate material, 440C HT stainless steel; load, 1 kg; estimated contact stress, 14 MPa (2000 psi); sliding speed, 2.6 m/sec; temperature, 25° C; atmosphere, moist air (10 000 ppm H₂O).

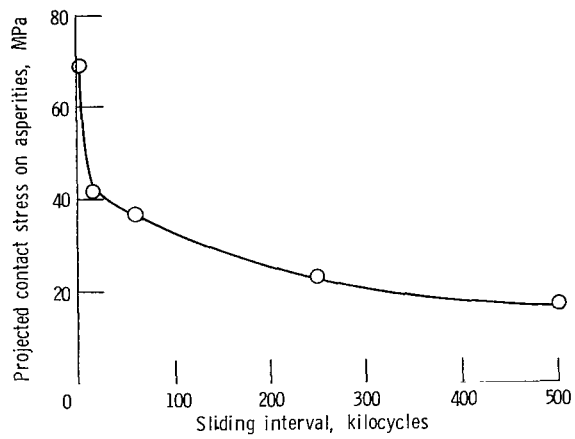
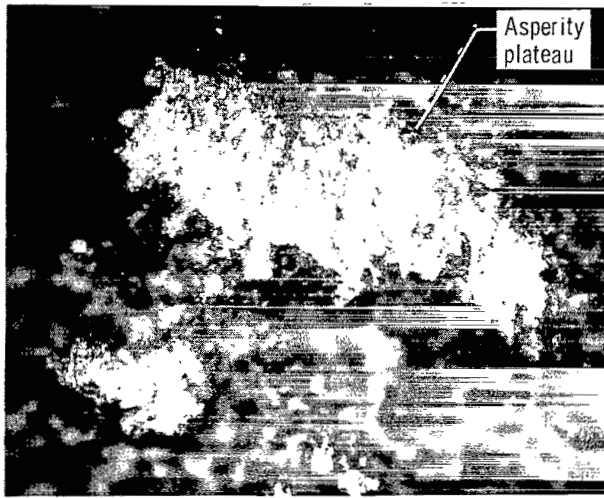
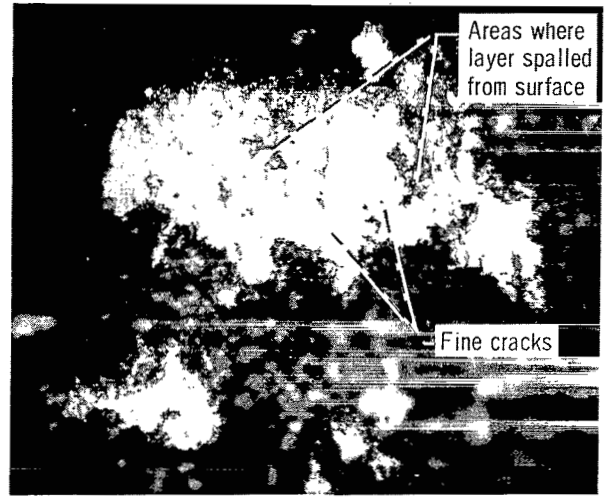


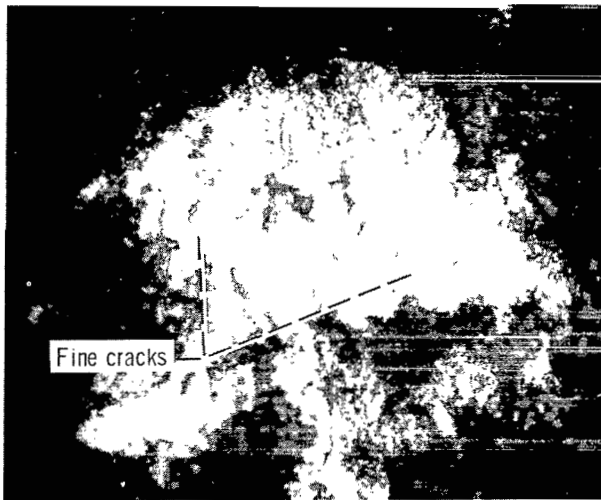
Figure 6. - Projected contact stress on asperities of polyimide-bonded graphite fluoride films as function of sliding interval. Rider and disk substrate material, 440C HT stainless steel; load, 1 kg on 0.95-mm-diameter flat on rider; sliding speed, 2.6 m/sec; temperature, 25^o C; atmosphere, moist air (10 000 ppm H₂O).



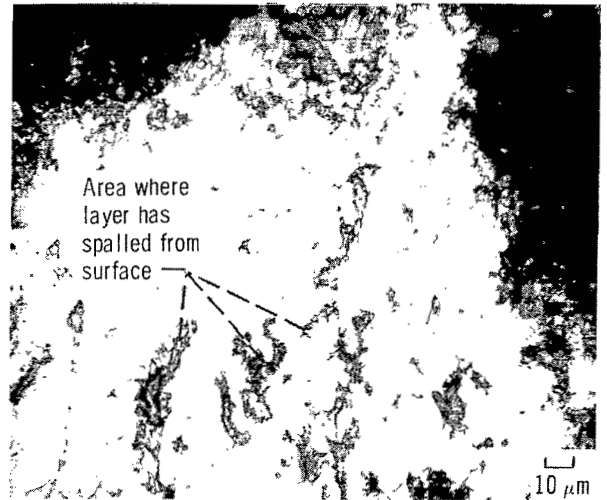
(a) Sliding interval, 1 kilocycle.



(b) Sliding interval, 15 kilocycles.

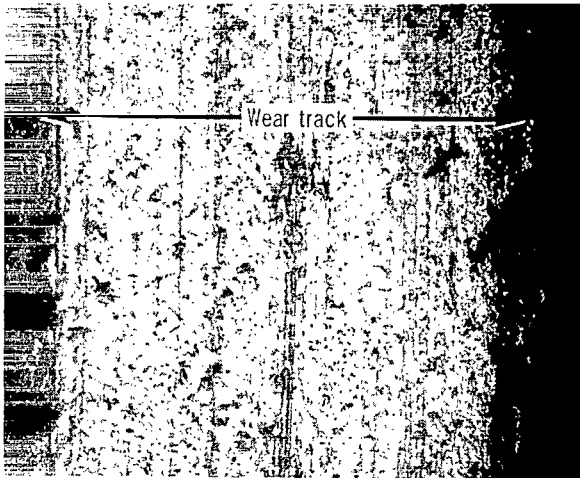


(c) Sliding interval, 60 kilocycles.

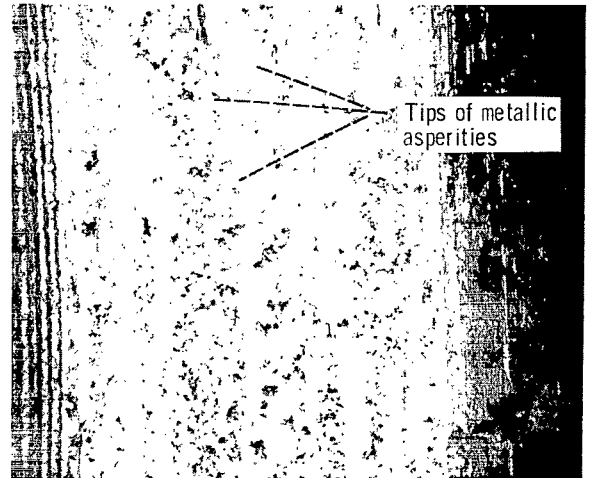


(d) Sliding interval, 250 kilocycles.

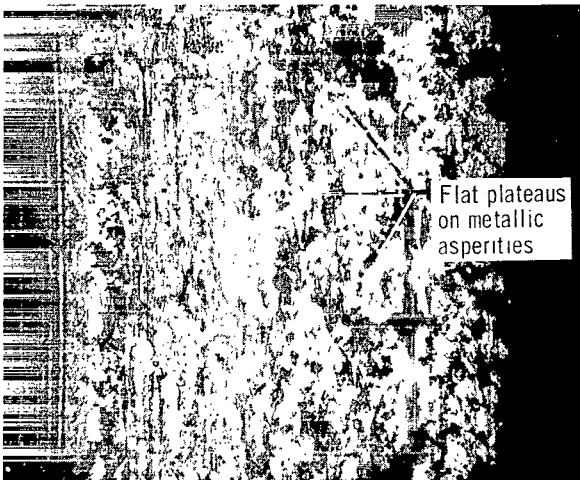
Figure 7. - High-magnification photomicrographs showing wear progression on polyimide-bonded graphite fluoride asperity plateau. Rider and disk substrate material, 440C HT stainless steel; load, 1 kg; estimated contact stress, 14 MPa (2000 psi); sliding speed, 2.6 m/sec; temperature, 25° C; atmosphere, moist air (10 000 ppm H₂O).



(a) Sliding interval, 1500 kilocycles.



(b) Sliding interval, 3500 kilocycles.

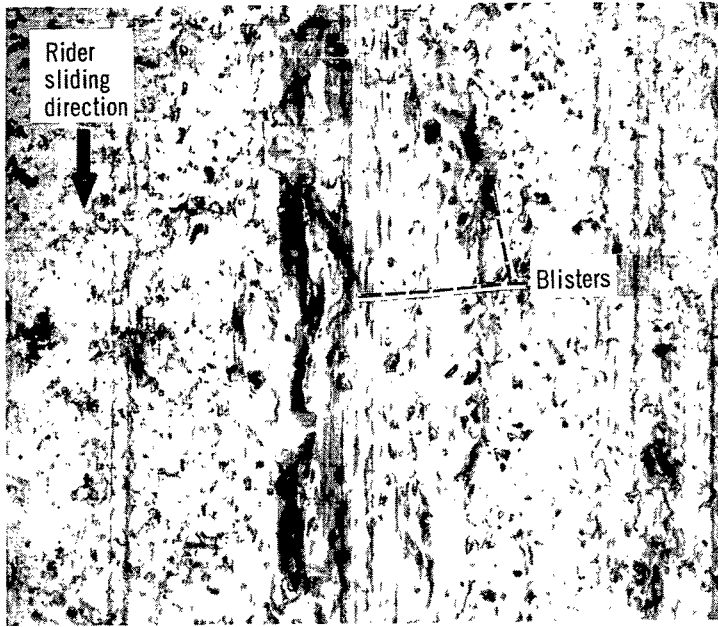


(c) Sliding interval, 6000 kilocycles.

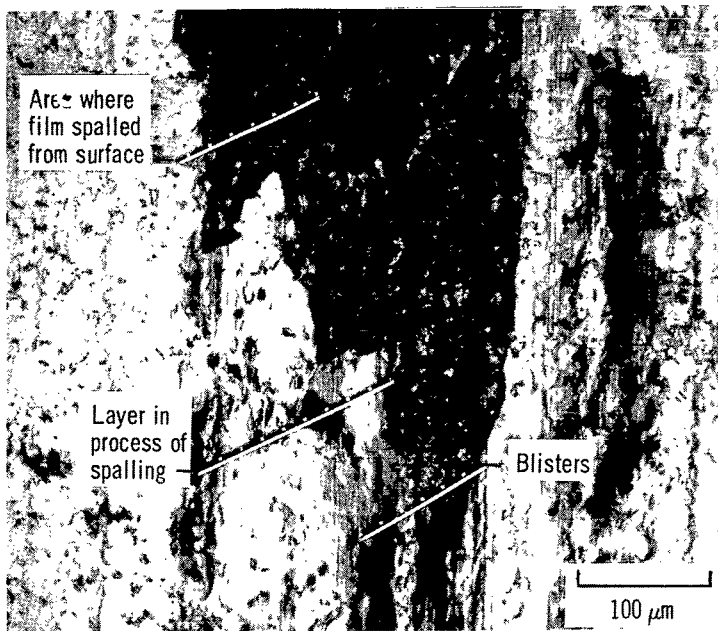


(d) Sliding interval, 8500 kilocycles.

Figure 8. - Photomicrographs of wear tracks on polyimide-bonded graphite fluoride films after long sliding intervals. Rider and disk substrate material, 440C HT stainless steel; load, 1 kg; estimated contact stress, 14 MPa (2000 psi); sliding speed, 2.6 m/sec; temperature, 25° C; atmosphere, moist air (10 000 ppm H₂O).

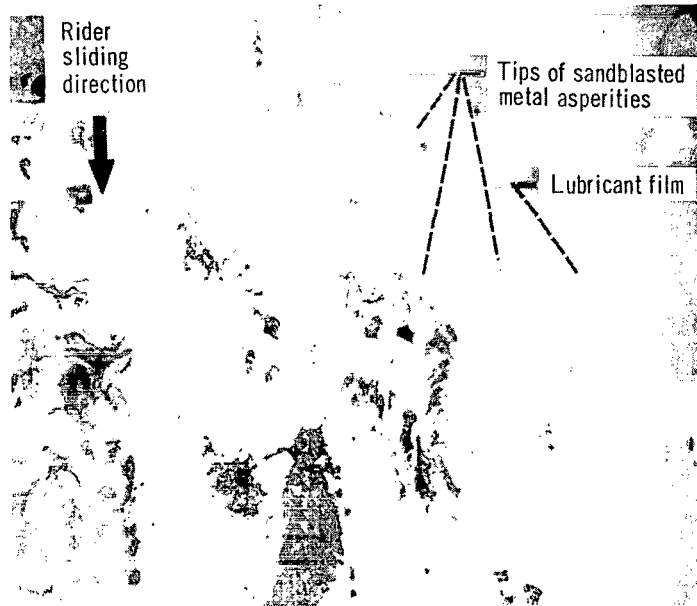


(a) Blistering.

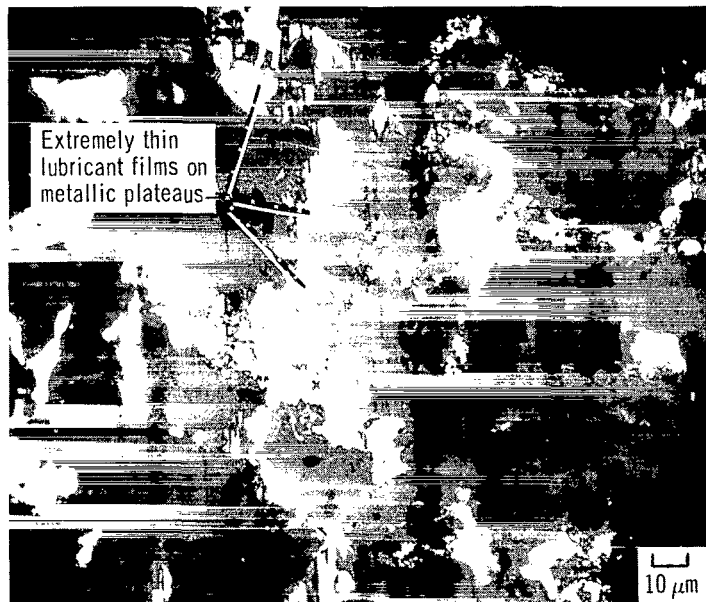


(b) Spalling of thin layers of film.

Figure 9. - Photomicrographs of areas on polyimide-bonded graphite fluoride film wear track after 1500 kilocycles of sliding, showing blistering and spalling of thin layers of film. Rider and disk substrate materials, 440C HT stainless steel; load, 1 kg; estimated contact stress, 14 MPa (2000 psi); sliding speed, 2.6 m/sec; temperature, 25° C; atmosphere, moist air (10 000 ppm H₂O).



(a) Sliding interval, 3500 kilocycles.



(b) Sliding interval, 8500 kilocycles.

Figure 10. - High-magnification photomicrographs of wear tracks shown in figure 8 after 3500 and 8500 kilocycles of sliding. Rider and disk substrate materials, 440C HT stainless steel; load, 1 kg; estimated contact stress, 14 MPa (2000 psi); sliding speed, 2.6 m/sec; temperature, 25° C; atmosphere, moist air (10 000 ppm H₂O).

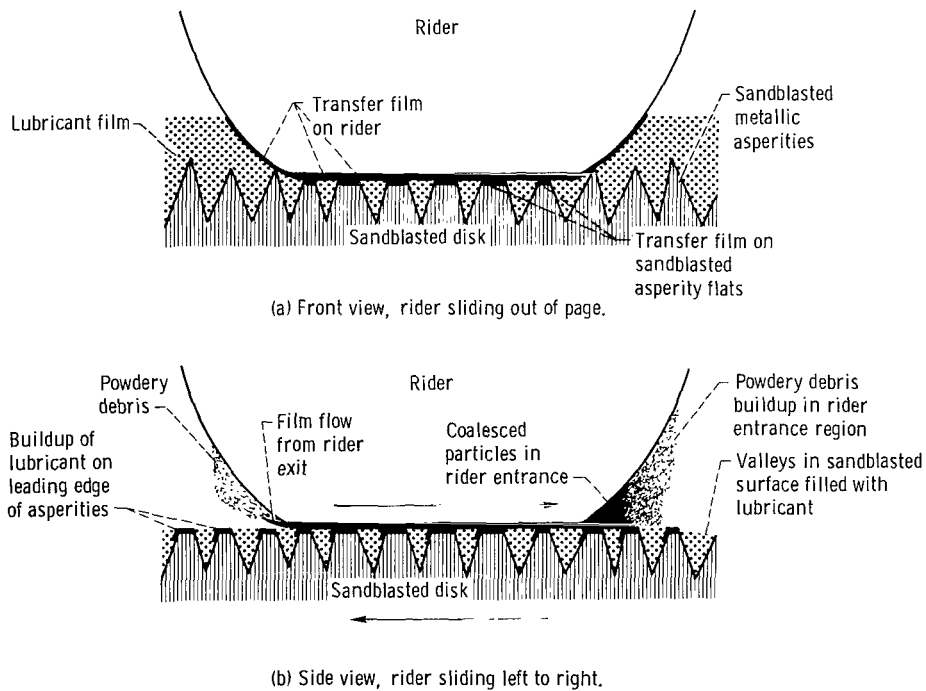
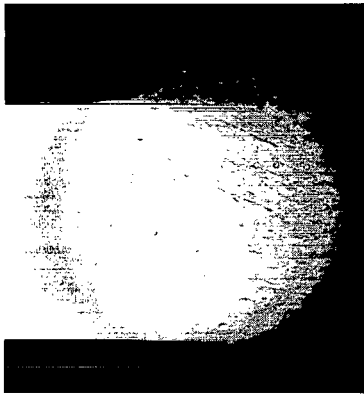
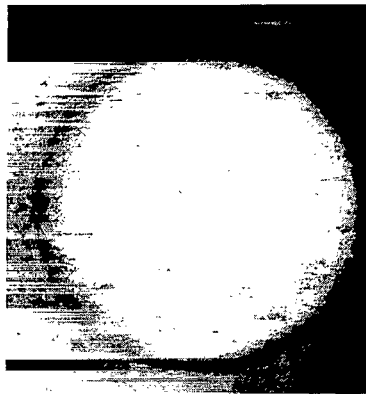


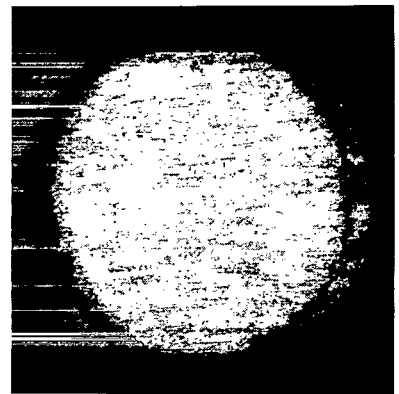
Figure 11. - Idealized schematic drawing of sliding surfaces, illustrating lubricating mechanism in the second stage of lubrication.



(a) Flat before sliding.



(b) Flat after 1 kilocycle of sliding.



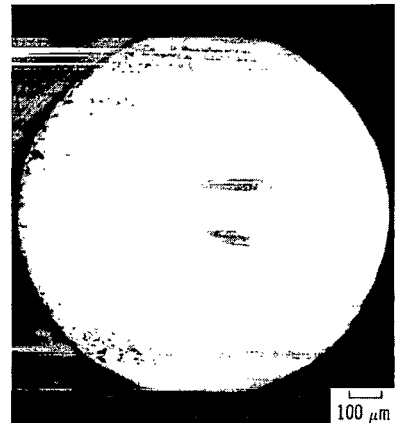
(c) Flat after 250 kilocycles of sliding.



(d) Flat after 1500 kilocycles of sliding.

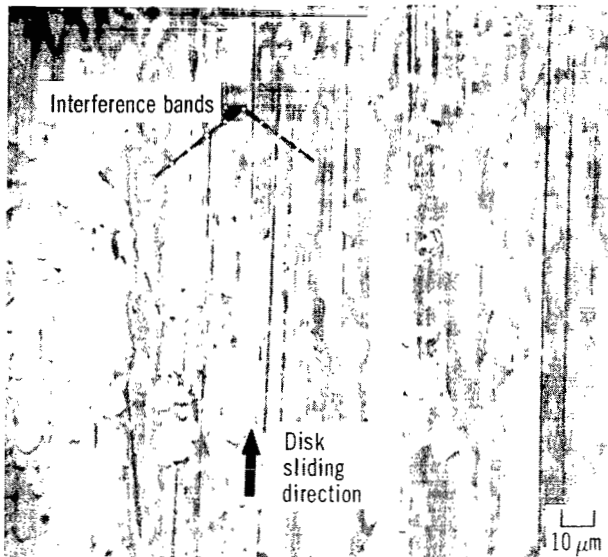


(e) Flat after 4500 kilocycles of sliding.

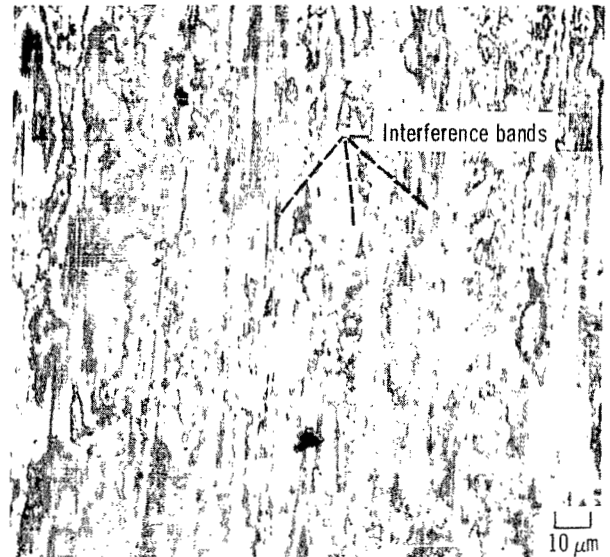


(f) Flat after 8500 kilocycles of sliding.

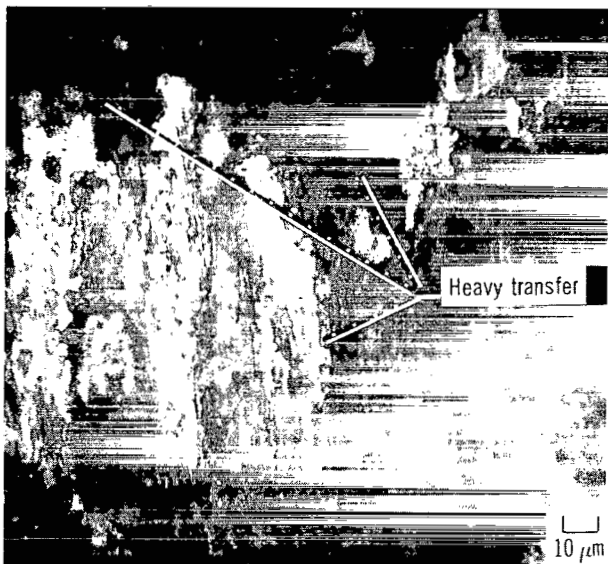
Figure 12. - Photomicrographs of 440C HT stainless-steel rider contact area after various intervals of sliding on polyimide-bonded graphite fluoride films. Disk substrate material, 440C HT stainless steel; load, 1 kg; estimated contact stress, 14 MPa (2000 psi); sliding speed, 2.6 m/sec; temperature, 25 °C; atmosphere, moist air (10 000 ppm H₂O).



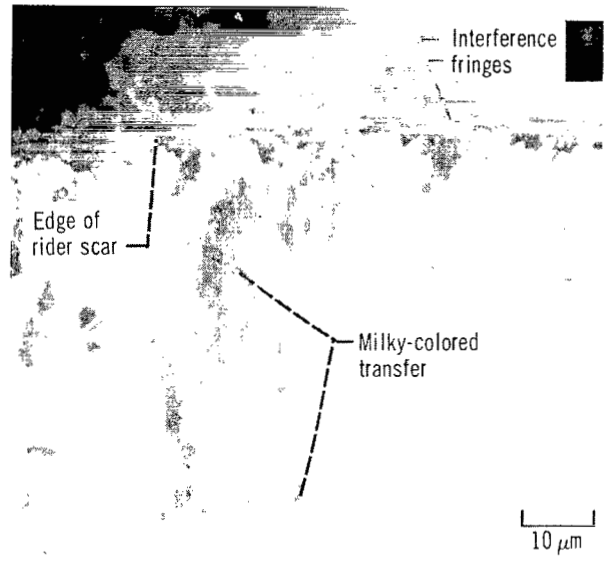
(a) Middle of scar (after 1 kilocycle).



(b) Middle of scar (after 250 kilocycles).



(c) Middle of scar (after 2500 kilocycles).



(d) Entrance area (after 8500 kilocycles).

Figure 13. - High-magnification photomicrographs of typical transfer to rider after various intervals of sliding on polyimide-bonded graphite fluoride films. Rider and disk substrate material, 440C HT stainless steel; load, 1 kg; estimated contact stress, 14 MPa (2000 psi); sliding speed, 2.6 m/sec; temperature, 25°C; atmosphere, moist air (10 000 ppm H₂O).

1. Report No. NASA TP-1584	2. Government Accession No.	3. Recipient's Catalog No.
4. Title and Subtitle LUBRICATION AND WEAR MECHANISMS OF POLYIMIDE-BONDED GRAPHITE FLUORIDE FILMS SUBJECTED TO LOW CONTACT STRESS	5. Report Date January 1980	6. Performing Organization Code
	8. Performing Organization Report No. E-9990	10. Work Unit No. 505-04
7. Author(s) Robert L. Fusaro	11. Contract or Grant No.	13. Type of Report and Period Covered Technical Paper
9. Performing Organization Name and Address National Aeronautics and Space Administration Lewis Research Center Cleveland, Ohio 44135	14. Sponsoring Agency Code	
	12. Sponsoring Agency Name and Address National Aeronautics and Space Administration Washington, D.C. 20546	
15. Supplementary Notes		
16. Abstract <p>The tribological properties of polyimide-bonded graphite fluoride films were studied with a pin-on-disk friction apparatus. But instead of the conventional hemispherically tipped rider, a 440C HT stainless-steel rider with a 0.95-millimeter-diameter flat area was slid against the film. This was done so that a lighter, more closely controlled contact stress could be achieved. A 1-kilogram load was applied to this flat to give a projected contact stress of 14 megapascals (2000 psi). As for a hemispherically tipped rider under the same load, two stages of lubrication were operating. In the first stage, the film supported the load and the lubricating mechanism appeared to be the shear of a thin surface layer of the film between the rider and the bulk of the film. The second stage began after the original film was worn away, and the lubricating mechanism appeared to be the shear of very thin lubricant layers between the flat area on the rider and flat plateaus generated on the sandblasted asperities of the metallic substrate. The major difference between the lubricating mechanisms of the hemispherical and flat riders was that the flat wore through the film much more slowly than did the hemisphere.</p>		
17. Key Words (Suggested by Author(s)) Lubricating mechanisms; Wear mechanisms; Polyimide; Graphite fluoride; Transfer films; Solid lubricant; Bonded film	18. Distribution Statement Unclassified - unlimited STAR Category 27	
19. Security Classif. (of this report) Unclassified	20. Security Classif. (of this page) Unclassified	21. No. of Pages 26
		22. Price* A03

* For sale by the National Technical Information Service, Springfield, Virginia 22161

National Aeronautics and
Space Administration

Washington, D.C.
20546

Official Business

Penalty for Private Use, \$300

THIRD-CLASS BULK RATE

Postage and Fees Paid
National Aeronautics and
Space Administration
NASA-451



13 1 1U,C, 120379 S00903DS
DEPT OF THE AIR FORCE
AF WEAPONS LABORATORY
ATTN: TECHNICAL LIBRARY (SUL)
KIRTLAND AFB NM 87117

NASA

POSTMASTER: If Undeliverable (Section 158
Postal Manual) Do Not Return
